The best known transformation is the "Prandtl stretching" defined, for small ε, by

$$x \to x: \quad y \to \varepsilon y: \quad u \to u: \quad v \to \varepsilon v: \quad \varepsilon^2 \equiv 1/R \neq 0 \qquad (5)$$

The transformation preserves the form of the equations and the coefficient of u_{yy} in Eq. (1) becomes unity. This "stretching" has been thoroughly discussed elsewhere.'

Birkhoff[2] suggests the following one parameter group:

$$x \to \beta^2 x: \quad y \to \beta y: \quad u \to u: \quad v \to \beta^{-1} v \qquad (6)$$

Under this transformation the form of Eqs. (1) and (2) is preserved with all terms having a multiplying factor of $1/\beta^2$. Thus for $\beta \neq 0$ or ∞ the group defined by Eq. (6) leaves the boundary-layer equations invariant.

Finally we discuss the general four-parameter group[2] described by

$$x \to \alpha x: \quad y \to \beta y: \quad u \to \gamma u: \quad v \to \delta v \qquad (7)$$

Birkhoff discusses the application to flow past an infinite wedge for which $U = cx^m$. This analysis reduces the boundary-layer equations to the usual Falkner-Skan ordinary differential equation. We are interested in generalized flow around a cylinder of the form

$$U = m \sin x \qquad (8)$$

We wish to know for what subgroups of (7) the boundary-layer equations are invariant with respect to variations in m. We also wish to preserve the form of U. Transforming the equations by means of (7) and equating the coefficients of different terms in each equation it is found that

$$\alpha = 1: \quad \beta = 1/m^{1/2}: \quad \gamma = m: \quad \delta = m^{1/2} \qquad (9)$$

where $m \neq 0, \infty$. Thus the required transformation is a one-parameter subgroup of (7) uniquely defined by

$$x \to x: \quad y \to y/m^{1/2}: \quad u \to mu: \quad v \to m^{1/2} v \qquad (10)$$

It is worth noting that $u_y \to m(m)^{1/2} u_y$. These results have the following application. It is often useful to be able to compare the boundary-layer solutions of different workers who have used different values of m for the external flow. The transformation (10) gives the scaling that must be used on the coordinates and velocities to compare solutions that have different m values. Typical values are $m = 1$ for Terrill's solution (Ref. 3) and $m = 2$ for Schonauer's solution (Ref. 4). The velocity profiles, at $x = 1.0$, obtained from Refs. 3 and 4 are compared by plotting u/U vs $y/m^{1/2}$ on Fig. 1. It is seen that the two solutions fall on the same curve, confirming the prediction of Eq. (10).

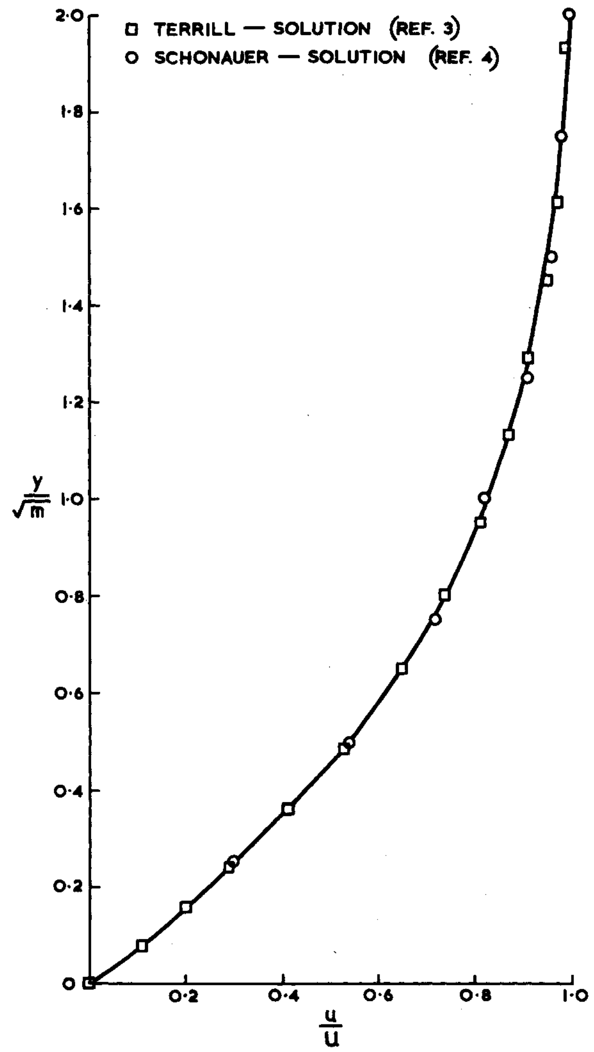

Fig. 1 Boundary-layer velocity profile for potential flow past a cylinder. Terrill and Schonauer solutions at $x = 1.0$.

References

[1] Van Dyke, M., *Perturbation Methods in Fluid Mechanics*, Academic Press, New York, 1964.

[2] Birkhoff, G., *Hydrodynamics*, Oxford University Press, 1960.

[3] Terrill, R. M. "Laminar Boundary Layer Flow Near Separation with and without Suction," *Philosophical Transactions of the Royal Society (London)*, A 253, 1960, pp. 55–100.

[4] Schonauer, W., "Differenzenverfahren zur Losung der Grenzschichtgleichung," *Inganieur-Archiv*, Vol. 33, 1964, pp. 173–189.

Buckling and Vibration Analysis for Stiffened Orthotropic Shells of Revolution

V. SVALBONAS* AND T. BALDERES†
Grumman Aerospace Corporation, Bethpage, New York

Introduction

THE multistep integration method has proven to be a usefı and versatile approach in the analysis of rotationall symmetric shells. The present Note provides a numerical methoı using the multistep integration approach, in which the bucklir and vibration analyses are formulated as a succession of line eigenvalue problems. The new method has some definite adva tages over the previous ones.[1] An estimate of the eigenvect is not required, and once an eigenvalue has been converg good estimates for other eigenvalues are automatically availabl This is accomplished through the use of an in-core Household scheme for solution of the eigenvalue problem. Furthermoı since the method uses an eigenvalue solution, the possibility missing modes is eliminated.

Formulation

The shell is considered as being made up of a series of se ments, having prescribed lengths, which are connected alo

Received December 15, 1971; revision received February 29, 19' Financial support was partly provided by NASA MSFC unc Contract NAS8-27468.

Index categories: Structural Stability Analysis; Structural Dynan Analysis.

* Structural Methods Engineer.

† Structural Methods Engineer. Associate Member AIAA.

Table 1 Over-all buckling of reinforced cylinder ($n = 0$)

Root no.	m	NASA TND 2960	NASA CR 1280	Current Method (20 segments)			
				Trial$_1$ (1×10^3)	Trial$_2$ (6017.0)	Trial$_3$ (5841.0)	Trial$_4$ (5848.0)
1 = crit.	13	5848.15	5842.9	6017.77	5840.9	5848.3	5848.01
2	14	5877.97	5872.2	6073.60	5871.1	5879.6	5879.22
3	12	5974.05	5968.4	6126.76	5972.4	5978.8	5978.56
4	15	6032.72	6025.6	6264.54	6033.4	6043.1	6042.75
5	16	6290.95	6281.6	6445.00	6308.4	6315.4	6315.67
6	11	6301.05	6293.9	6569.61	6310.3	6319.6	6319.13
7	17	6637.3	6624.8	6971.53	6683.3	6695.9	6695.42
8	10	6898.31	6888.4	7040.98	6923.9	6928.9	6928.68
9	18	7060.56	7044.1	7448.06	7148.8	7162.6	7162.07
10	19	7552.39	7530.9	7940.50	7691.5	7704.7	7704.21
11	9	7875.44	7861.1	8023.79	7923.9	7928.1	7927.93
12	20	8106.50	8078.8	9574.56	8639.5	8683.2	8681.50
13	21	8718.03		9821.53	9180.8	9214.4	9213.05
14	22	9383.22		10196.41	9492.9	9496.4	9496.24
15	8	9414.65	9393.2	11002.30	10005.7	10039.9	10038.53
16	23	10099.1		12008.57	10949.3	10986.6	10985.08
17	24	10863.3		12010.31	11950.2	11952.7	11952.57
18	25	11674.00		13167.73	12009.9	12051.4	12049.73

common junctions called joint lines. Stiffness and load coefficients of these segments are obtained by applying a Runge-Kutta numerical procedure to integrate the shell differential equations. By properly combining these coefficients the stiffness and load matrices of the entire shell are formed. Inasmuch as the circumferential Fourier harmonics are uncoupled for a linear analysis of shells of revolution, the stiffness matrix, which relates joint forces, $\{F\}$, to joint displacements, $\{\Delta\}$, is uncoupled, and we can write for the nth harmonic

$$\{F\}^{(n)} = \{K_0\}^{(n)}\{\Delta\}^{(n)} + \{L\}^{(n)} \tag{1}$$

A solution for the static problem is obtained by solving the above set of equations for the joint displacements under a given applied load distribution. These displacements are then used to obtain the stress resultants throughout the shell.[2]

This formulation is extended to stability and free vibration analyses by including the effects of applied loads and shell inertia in the stiffness of the shell, and omitting the load vector. For stability analysis this is done by adding nonlinear terms involving products of in-plane loads and shell rotations to the basic shell equilibrium equations.[3,4] The in-plane resultants are obtained by first solving the statics problem under the given applied loads. The numerical integration procedure is then used on the new set of shell equations, which include the nonlinear effects, to form a modified stiffness matrix $[K_T]^{(n)}$. This matrix, called the total stiffness matrix, relates increments of forces $[F']$ to increments of displacements $\{\Delta'\}$. Next the principle of virtual work is used to obtain the condition for stability

$$[K_T]^{(n)}\{\Delta'\}^{(n)} = \{0\} \tag{2}$$

For free vibration analysis dynamic terms which account for the inertia of the shell are included in the differential equations. Application of the numerical integration procedure results again in Eq. (2), where the stiffness matrix $[K_T]^{(n)}$ now includes the dynamic terms.

The solution of a homogeneous set of equations as (2) is often obtained by the determinant method.[4] An alternate solution was presented using a modified Stodola method.[3] The drawbacks of these procedures were mentioned earlier. The current procedure works by reformulating the solution of Eq. (2) into a succession of linear eigenvalue problems. Reformulation of the problem is accomplished by splitting $[K_T]^{(n)}$ into two parts. The first part is the standard elastic stiffness matrix, $[K_0]^{(n)}$, while the second part represents the change in the stiffness due to the in-plane loads (for the buckling problem) or the inertia terms (for the free vibration problem). This second part is obtained by simply substracting the $[K_0]^{(n)}$ stiffness from the total stiffness $[K_T]^{(n)}$, thus:

$$[K_P]^{(n)} = [K_T]^{(n)} - [K_0]^{(n)} \tag{3}$$

Note that $[K_P]^{(n)}$ is a function of the prestress or of the frequency, and that this transcendental functional dependence is not explicity defined. Hence, $[K_P]^{(n)}$ can only be formed for a specific value of prestress or frequency. Having formed $[K_P]^{(n)}$ and $[K_0]^{(n)}$, the solution of Eq. (2) can be formulated as a linear eigenvalue problem requiring an iterative solution:

$$[K_T]^{(n)}\{\Delta'\} = \left[\{K_0\}^{(n)} + (\lambda_i/\lambda_{i-1})[K_P(\lambda_{i-1})]^{(n)}\right]\{\Delta'\}^{(n)} = \{0\} \tag{4}$$

where λ_i is the sought eigenvalue.

In Eq. (4) it is recognized that $[K_T]^{(n)}$ is not a linear function of the eigenvalue, however, a linear assumption has been found to be a good approximation in an iterative procedure. Having formed $[K_0]^{(n)}$ and $[K_P]^{(n)}$ for a particular value of λ_0, the linear eigenvalue problem in Eq. (4) is solved for the ratio λ_1/λ_0 assuming $[K_P]^{(n)}$ as constant. Then using λ_1, $[K_P(\lambda_1)]^{(n)}$ is computed, and Eq. (4) is solved again for λ_2/λ_1. This process is repeated until the ratio λ_i/λ_{i-1} equals unity, making Eq. (4) exact, and λ_i a solution. It should be noted that in the above procedure an eigenvalue formulation is obtained by separating $[K_P]^{(n)}$ from $[K_T]^{(n)}$ by subtraction. This is in contrast to the usual formulation of linear eigenvalue problems where each matrix can be formed independently.

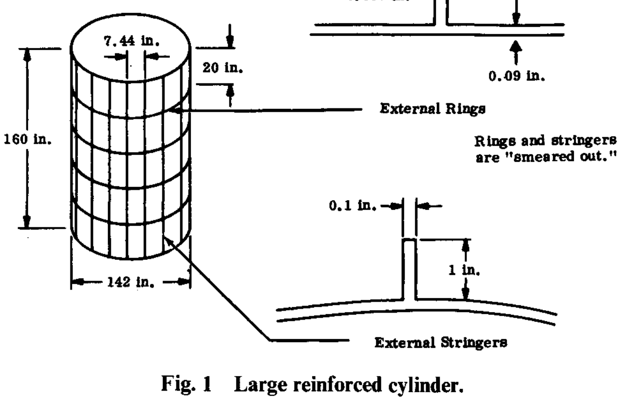

Fig. 1 Large reinforced cylinder.

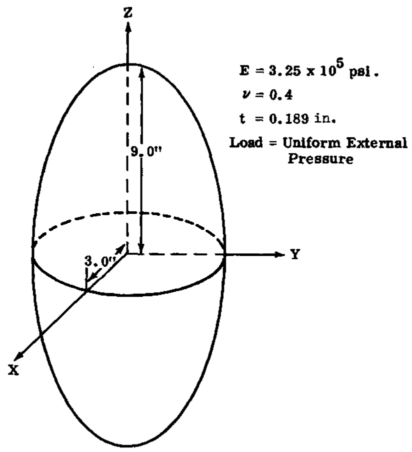

Fig. 2 Axisymmetrically pressurized prolate spheroid.

Numerical Examples

The use of the method is demonstrated by its application to two shell buckling problems presented below. The first problem involves a large, ring-stringer eccentrically reinforced cylinder (Fig. 1).‡ The loading was a fixed internal stabilizing pressure of 31 psi, in combination with a variable compressive end load. Classical simple support boundary conditions were utilized to enable comparison with Refs. 6 and 7. The idealization used consisted of 20 segments for the whole structure. Comparisons of the analytical results are presented in Table 1. The over-all critical mode was found to be $n = 0$, $m = 13$, where n is the number of circumferential waves and m the number of longitudinal half-waves. Table 1 shows the analytical results for the $n = 0$ calculations, and it can be seen again that the convergence characteristics are excellent. By the fourth pass, the change from anticipated to corrected value of the critical load is only 0.00017%, moreover, the estimates of some of the higher eigenvalues show an average difference of 0.57% (with a maximum of 2.0%) for the first 11 roots, and an average difference of 2.72% (with a maximum of 10%) for the first 18 roots, when compared to Ref. 7. Thus, when the first root is converged, excellent estimates are available for a large number of the higher roots. The results from Refs. 6, 7 and the current work should be close, but do not have to agree exactly, due to differences in shell theories and formulations. No difficulty was encountered in obtaining eigenvalues corresponding to eigenvectors with many waves in a segment or with load reversals.

The second problem considered is a prolate spheroidal shell under a uniform external pressure as shown in Fig. 2. The results obtained with the present approach are compared to experimental and other theoretical results in Table 2. It can be seen that the results from the three numerical integration techniques are all very close to the experimental predictions.

Table 2 Comparison of results for prolate spheroid

Harmonic shape	Buckling load, psi		
	$n = 2$	$n = 3$	$n = 4$
Current method	208.3	138.39	174.1
Experimental (Ref. 8)	—	137.0	—
Theoretical (Ref. 8)	> 197.0	> 197.0	197.0
Ref. 3	208.8	138.7	174.0
Ref. 4	—	139.23	—

‡ Notes on Fig. 1: Loading—compressive end load is N, internal stabilization pressure is 31 psi; Boundary conditions—ends are simply supported.

References

[1] Svalbonas, V. and Balderes, T., "A Procedure for Extending the STARS II Digital Computer Program to Shell Buckling Analysis," Grumman ADN 02-01-71.1, May 1971.

[2] Svalbonas, V., "Numerical Analysis of Shells—Vol. I: Unsymmetric Analysis of Orthotropic, Reinforced Shells of Revolution," CR-61299, Sept. 1969, NASA.

[3] Cohen, G., "Computer Analysis of Asymmetric Buckling of Ring Stiffened Orthotropic Shells of Revolution," AIAA Paper 67-109, New York, Jan. 1967.

[4] Kalnins, A., "Static, Free Vibration, and Stability Analysis of Thin, Elastic Shells of Revolution," AFFDL-TR-68-144, March 1969, Wright-Patterson Air Force Base, Ohio.

[5] Hurty, W. and Rubinstein, M., *Dynamics of Structures*, Prentice-Hall, Englewood Cliffs, N.J., 1965.

[6] Dickson, J. and Brolliar, R., "The General Instability of Eccentrically Stiffened Cylindrical Shells under Axial Compression and Lateral Pressure," CR-1280, Jan. 1969, NASA.

[7] Block, D., Card, M., and Mikulas, M., "Buckling of Eccentrically Stiffened Orthotropic Cylinders," TN D-2960, Aug. 1965, NASA.

[8] Hyman, B. and Healey, J., "Buckling of Prolate Spheroidal Shells under Hydrostatic Pressure," *AIAA Journal*, Vol. 5, No. 8, Aug. 1967, pp. 1469–1477.

Effect on Supersonic Jet Noise of Nozzle Plenum Pressure Fluctuations

RAYMOND KUSHIDA* AND JACK RUPE†
Jet Propulsion Laboratory, Pasadena, Calif.

THE proportion of the total engine noise which is attributable to the jet plume in a jet propulsion device increases markedly as the exhaust velocity increases.[1] When the jet velocity is nearly sonic or supersonic, then the jet noise can overwhelm other noise sources. In this preliminary study it is found that the interaction of upstream disturbance with a supersonic jet plume causes an increase in the total noise. It is expected that this added insight into jet noise sources will be useful in devising improved methods of noise reduction in future jet engines.

The noise radiated from a supersonic jet plume was measured and the sound power was correlated with the pressure fluctuations measured in the chamber. A research liquid rocket engine using the propellant combination hydrazine and nitrogen tetroxide was used to generate a wide range of chamber pressure fluctuation. Previous experience at JPL with that propellant combination had shown that very smooth combustion could be

Table 1 Rocket engine geometric characteristics

Length (injector to throat)	1.17 m (46 in.)
Chamber diameter	0.28 m (11 in.)
Nozzle throat diameter	0.197 m (7.76 in.)
Throat wall cuvature radius	0.199 m (7.84 in.)
Nozzle exit diameter	0.228 m (8.95 in.)
Nozzle divergence half angle	15°

Received December 30, 1971; revision received March 14, 1972. This paper represents the results of one phase of research carried out at the Jet Propulsion Laboratory, California Institute of Technology under Contract NAS7-100 sponsored by NASA.

Index categories: Aircraft Propulsion System Noise; Liquid Rocket Engines; Jets, Wakes, and Viscid-Inviscid Flow Interactions.

* Member of the Technical Staff, Liquid Propulsion Combustion Research Group.

† Supervisor, Liquid Propulsion Combustion Research Group.